https://doi.org/10.5194/egusphere-2025-6432
Preprint. Discussion started: 4 January 2026

Automated UAV systems for geohazard monitoring: case studies from the Supphellebreen icefall (Norway), the Skjøld instability (Norway), and the Blatten landslide (Switzerland)

Alexander Maschler[1], Sarah Langes[1], Lukas Schild[1], Thomas Scheiber[1], Paula Snook[1], Jacob Clement Yde[1], Harald Zandler[2], Ueli Sager[3]

[1] Department of Civil Engineering and Environmental Sciences, Western Norway University of Applied Sciences, Sogndal, Norway
[2] Department of Geography and Regional Science, University of Graz, Graz, Austria
[3]Remote Vision, Switzerland

Correspondence to: Alexander Maschler, alexander.maschler@hvl.no

Abstract

This study presents the first systematic field evaluation of dock-based UAV (Uncrewed Aerial Vehicle) systems for geohazard monitoring in mountainous terrain. We tested their potential across three different environments: (1) a fast-moving glacier icefall (Supphellebreen, Norway), (2) an unstable rock slope (Skjøld, Norway), and (3) a post-failure landscape resulting from a catastrophic rock-ice avalanche (Blatten, Switzerland). Effective hazard management requires timely detection of displacement patterns and terrain change. To address these issues, we introduce an automated workflow integrating multitemporal UAV dock data acquisition with an end-to-end processing pipeline for displacement field generation and change detection. The results show that this workflow has the potential to provide data at centimetre-level accuracy before, during, and after hazard events, supporting both precautionary risk assessments and timely decision-making in critical phases of potential hazard evolution. Wider adoption will depend on supportive regulatory frameworks, reliable power and communication infrastructure, and sufficient expertise to ensure effective operation, maintenance, data interpretation and risk management. Overall, dock-based UAV systems represent a significant technological advancement in efficient geohazard monitoring, facilitating rapid response in critical situations, thereby contributing to increased resilience of communities living in vulnerable mountain environments.

1 Introduction

Unstable rock slopes and glacier hazards such as ice avalanches, glacier collapse, and glacier lake outburst floods pose significant risks in mountainous regions, with increasing activity driven by climate change (Stoffel et al., 2024; Stuart-Smith et al., 2021). The growing threat of these natural hazards, that can potentially develop into multi-hazard cascades with catastrophic consequences, emphasizes the necessity for highly flexible monitoring and continuous risk assessments (Clague

https://doi.org/10.5194/egusphere-2025-6432
Preprint. Discussion started: 4 January 2026

et al., 2012; Klimeš et al., 2021; Picarelli et al., 2021; Zhong et al., 2025). Monitoring is often the only way to predict hazardous events in mountain environments and protect vulnerable communities living in these (Kristensen et al., 2021; Stähli et al., 2015).

Despite significant advances in remote sensing technologies, including terrestrial laser scanning, differential GNSS, InSAR, and camera systems, each technique faces distinct trade-offs regarding spatial coverage, temporal frequency, logistical feasibility, and line of sight (LoS) constraints (Dwivedi et al., 2016; Frodella et al., 2017; Huang et al., 2023; Schlögl et al., 2022). To overcome these challenges, Uncrewed Aerial Vehicles (UAVs) equipped with optical instruments are increasingly deployed in mountain environments as an extension of the existing geohazard monitoring toolkit (Gerstner et al., 2025; Lelli et al., 2025; Maschler et al., 2025; Rodriguez et al., 2020). Digital cameras carried by UAVs offer relatively high-resolution imagery and especially photogrammetric mapping has become relatively cheap. Yet, conventional UAV surveys remain largely manual and campaign-based, which is often limiting their frequency. Recent advancements in automated, semi-autonomous UAV technologies, such as base stations housing a UAV, often referred to as UAV docks or drone docks, enable operations to be carried out more frequently, also in remote areas, as they reduce the need for human intervention and access to hazardous sites. The design of such UAV systems allows for fully automated flight operations, including take-off, mission execution, flight abortion in an emergency, landing, charging, and wireless data transfer. In a previous study, a UAV system was tested in the context of detecting surface elevation changes for sediment monitoring in Switzerland (Walter et al., 2022). Although UAV docks represent a highly novel advancement in automated UAV technology, their potential to enhance geohazard monitoring in remote alpine environments is yet largely unexplored.

This study presents the first systematic field evaluation of a drone dock-based automated UAV system, coupled with a new automated workflow for displacement and change detection, and applied to three different settings in mountainous terrain. We demonstrate the potential of using a UAV dock for hazard monitoring and assessment of (1) a fast-moving glacier icefall, (2) a complex unstable rock slope, and (3) post-failure deposits from a catastrophic glacier collapse. By assessing its operational reliability, data quality, and monitoring capabilities under real-world conditions, this work addresses a critical gap in current research concerning the practical deployment and performance of automated UAV systems. Beyond visual inspection of hazardous sites, effective hazard management requires the ability to capture displacement patterns and track terrain changes in real time. To address this challenge, we introduce a novel workflow that integrates multitemporal data acquisition from UAV docks with an end-to-end processing pipeline for displacement field generation and change detection. The results from our three test sites demonstrate that UAV docks provide valuable highly spatially and temporally resolved data for pre-failure assessment of unstable slopes and glacier hazards, rapid-response mapping immediately after failure events, and situational awareness in the aftermath of catastrophic multi-hazard scenarios. Access for manual hazard evaluation in such environments is generally impossible due to high risk. We evaluate the feasibility and limitations of automated UAV technology, complemented by a brief accuracy assessment. Drawing on our operational experience, we highlight how automated monitoring can contribute to both research on mass movements and practical geohazard management. We identify current

https://doi.org/10.5194/egusphere-2025-6432
Preprint. Discussion started: 4 January 2026

challenges and provide recommendations on what is needed to advance automated monitoring networks in difficult to access and high-risk terrain.

2 Test sites & data

We tested our innovative monitoring approach, composed of a dock-based UAV system and an automated data processing workflow, at two locations in Norway and one location in Switzerland: (1) Supphellebreen is an outlet glacier of Jostedalsbreen ice cap, the largest ice mass in continental Europe; (2) Skjøld is a large and complex unstable rock slope in Vang municipality, Norway; and (3) at the Blatten locality in Lötschental, Switzerland, occurred a catastrophic ice-rock-debris avalanche in 2025. The terminal part of Supphellebreen consists of a fast-flowing icefall in steep and inaccessible terrain that makes conventional measurement campaigns and the installation of in situ instruments impractical and hazardous. The complex unstable mountain slope, Skjøld, covers over 1.4 km^2 and has displacement rates below 1 m a^{-1}. The terrain allows for implementing traditional in-situ instrumentation, which is, however, time-consuming and contains substantial risk due to the unstable nature of the site and frequent rockfalls. The third site, Blatten, represents a post-failure rock and ice avalanche scenario, where a UAV dock was successfully deployed for hazard mapping and risk assessment. Following the rock and ice avalanche event, the area remained inaccessible due to persistent instability, which prevented the use of conventional ground-based monitoring.
These three locations, chosen for their contrasting mass-movement characteristics and monitoring challenges, enable a critical assessment of our approach and allow us to evaluate the effectiveness of UAV docks and the workflow in both research and operational settings.

https://doi.org/10.5194/egusphere-2025-6432
Preprint. Discussion started: 4 January 2026

2.1 Supphellebreen - an outlet glacier of Jostedalsbreen ice cap, Norway

Supphellebreen (61°28'31.1"N 6°48'31.5"E) is an outlet glacier in the southern part of Jostedalsbreen ice cap in Fjærland, western Norway (Fig. 1). Its lower part is classified as a "regenerated glacier" because the glacier terminus is detached from the main glacier above (Fig. 1a). The regenerated lower part is fed by snow and ice avalanche activity from an icefall at the margin of the upper part of the glacier, and exists at a very low altitude of about 60 m asl; thereby, being the lowest glacier in Norway. The heavily crevassed icefall channels glacier ice at high flow velocities from an accumulation area that reaches up to 1690 m asl and has a maximum ice thickness of about 435 m (Gillespie et al., 2024) to a steep mountain slope where the ice dry-calves (Fig. 1b). Although no previous studies are available from Supphellebreen, it can be assumed that the ice flow velocity at the icefall is controlled by changes in ice thickness and the amount of subglacial meltwater. Temporal (diurnal and seasonal) variations in the basal sliding velocity and episodic acceleration during moderate to heavy rainfall events and high temperature ice-melt events can be observed. As a consequence of climate change, Supphellebreen has lost approximately 16% of its area since its maximum Little Ice Age extent in 1750 (Carrivick et al., 2022) and glacier change simulations indicate that Supphellebreen will undergo severe thinning and recession in the future, particularly from the last decades of the 21st century (Åkesson et al., 2025). Several glacier lake outburst floods (GLOFs) have occurred at Supphellebreen, where the most historically significant took place in 2004, when a GLOF originated from a moraine-dammed lake due to the breaching of a moraine ridge (Breien, 2008).

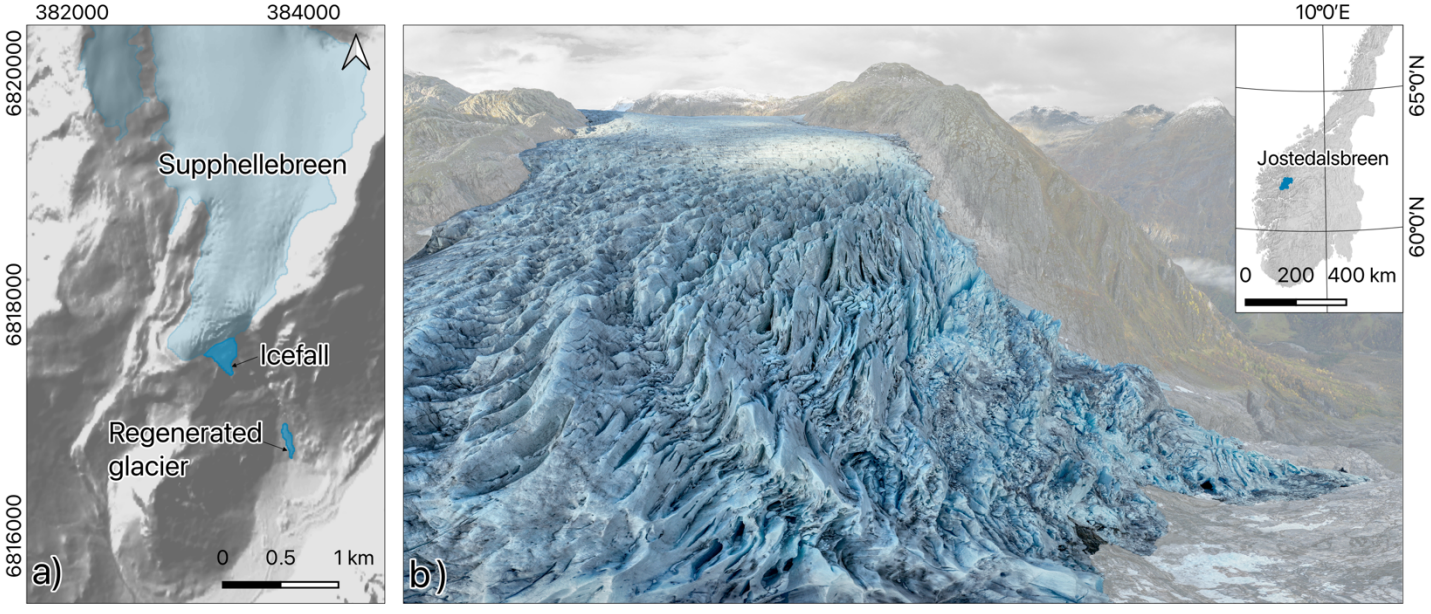

Figure 1 a) Overview map showing the location of Supphellebreen, the icefall and the regenerated glacier below. The monitored glacier areas are highlighted in blue. b) The aerial imagery shows the heavily crevassed icefall at 1000 m asl. Location of Jostedalsbreen in Norway (inset) Elevation data: © Kartverket

https://doi.org/10.5194/egusphere-2025-6432
Preprint. Discussion started: 4 January 2026

2.2 The complex unstable rock slope Skjøld in Vang municipality, Norway

The complex rock slope instability Skjøld (61°08'48.0"N 8°26'33.2"E), is situated south of lake Vangsmjøse in Vang Municipality, Norway (Fig. 2). The European Route E16 runs along the base of the slope, highlighting the potential hazard to infrastructure. The unstable area (1.4 km²) extends from an elevation of 670 m asl up to the summit of Bergsfjellet at 1585 m asl. A prominent 250-meter-high vertical cliff marks the upper boundary of the slope (Fig. 2b). The majority of the slope is covered by scree deposits, with block sizes ranging from 1 m^3 to 500 m^3 and is characterized by displacement rates of up to 0.75 m a^{-1}. Several distinctive rock "towers" are located in the upper part of the slope. Recent failures from the vertical top cliff occurred in October 2019 and 2021, with major deposition on the scree below and single boulders reaching beyond the foot of the scree deposits (NVE Atlas). In the western section, a well-defined rock slab with an estimated volume of >10^6 m^3 is bounded by up to 20 m wide open fractures and currently exhibits minimal displacement. However, due to its considerable volume and the potential runout distance, this section represents a significant hazard in case of potential future acceleration and failure scenarios. Frequent rockfall activity is observed across the slope throughout the year, with a marked increase during spring, likely associated with freeze-thaw cycles and snowmelt processes.

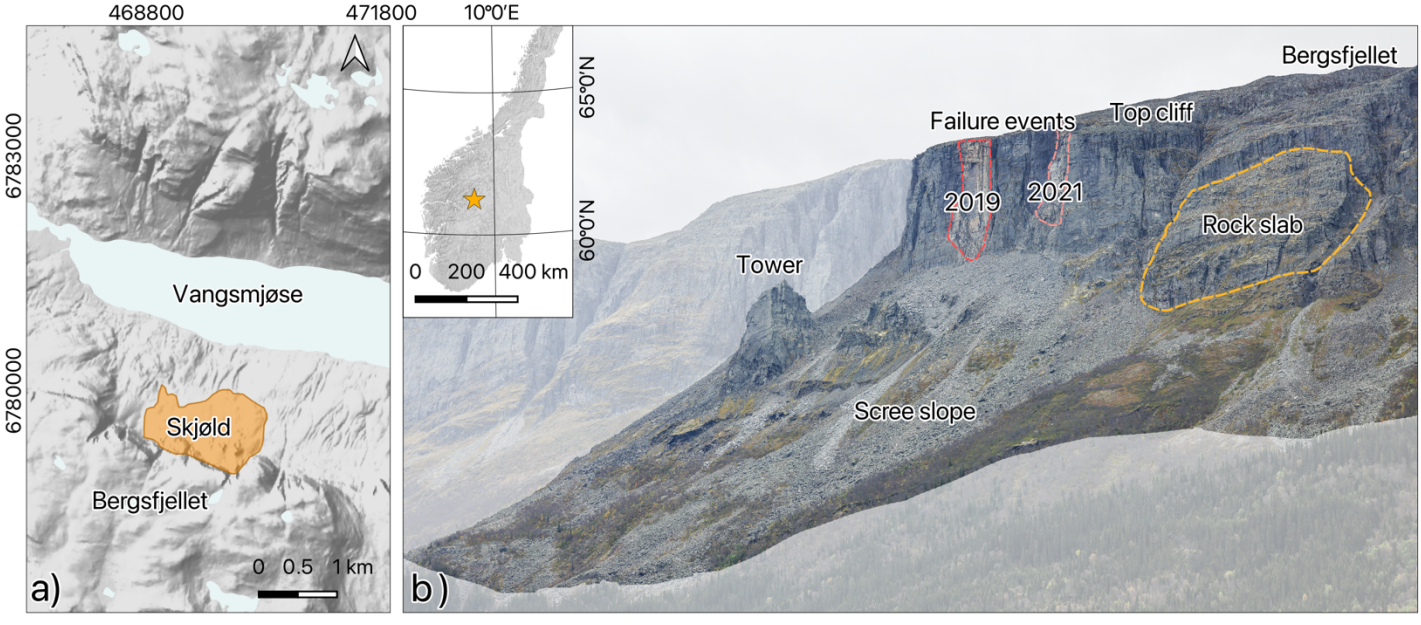

Figure 2 a) Location of the unstable rock slope Skjøld above Vangsmjøse and in eastern Norway (inset). b) Location of the main "tower" and the failure events from 2019 and 2021 (red outlines) and the rock slab (orange outline). Elevation data: © Kartverket

https://doi.org/10.5194/egusphere-2025-6432
Preprint. Discussion started: 4 January 2026

2.3 The multi-hazard cascade in Blatten, Lötschental in Valais, Switzerland

Following several rock slope failures from Kleines Nesthorn (Fig. 3) onto the underlying Birchgletscher (46°24'11.9" N, 7°50'11.8" E), the Birchgletscher collapsed catastrophically on 28 May 2025 (Büntgen et al., 2025). $9.57 \times 10^6 \pm 1.39 \times 10^5$ m^3 of rock and ice were deposited in Lötschental burying large parts of the village of Blatten (Yang et al., 2025). A UAV dock was rapidly deployed and automated UAV flights were carried out one day after the event until 18 November 2025 to monitor changes in the ice-containing landslide deposits, in the dammed or kettle lake formation, and to assist in ongoing hazard assessment and response efforts.

The upper part of Birchgletscher has been monitored due to two notable historic snow- and ice avalanche events in 1993 and 1999, that partially impacted local infrastructure. Since 2019, however, the lower part of the glacier front advanced approximately by 50 m related to acceleration of ice flow. Simultaneously, thinning of ice was observed in the upper reaches, while ice thickness at the lower part of the glacier increased by 30 m between 2011 and 2023 (Farinotti et al., 2025). This may be explained by accumulation of rock debris from periodic, pre-event rockfalls that insulated the glacier ice, reducing melting rates on the lower part of the glacier. Due to the enhanced thickening and moderate rainfall, the glacier front started to accelerate to 0.5 m per day in the days up to the glacier collapse (Islam et al., 2025). A combination of drivers led to the multi-hazard cascade on 28 May 2025. These likely included terrain motion due to partial collapse of the unstable Kleines Nesthorn lying within an area of probable permafrost, and rock debris accumulation medium on the glacier surface of the underlying

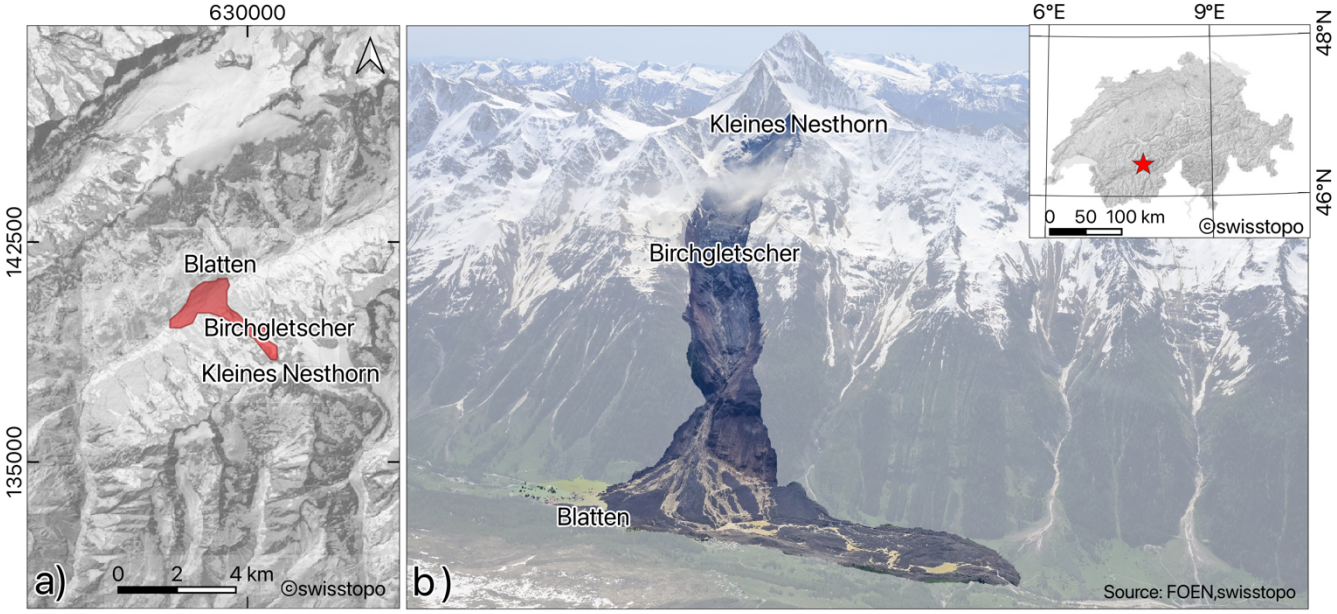

Figure 3 a) Map showing the location of the ice-rock-debris avalanche from Birchgletscher and Kleines Nesthorn in southwestern Switzerland (inset). b) Aerial photograph taken by the rapid mapping campaign (Source: FOEN, swisstopo) showing the extent of the failure event from 28 May 2025, destroying the village of Blatten. © Swisstopo

https://doi.org/10.5194/egusphere-2025-6432
Preprint. Discussion started: 4 January 2026

Birchgletscher (Farinotti et al., 2025). Furthermore, a strong increase in rock-ice thickness would cause pressure melting and speed-up of the sliding velocity of a temperate glacier. Consequently, Birchgletscher collapsed (i.e., the glacier front separated from the upper part of the glacier, disintegrated, and was displaced down-valley) and buried the village of Blatten (Büntgen et al., 2025). Local authorities issued an evacuation order for citizens to evacuate the village on 19 May 2025. Geohazard monitoring and timely early warning prior the catastrophic failure event facilitated the evacuation of around 300 residents with their livestock to nearby villages outside the hazard zone in Lötschental. The deposits dammed the river Lonza and created a lake which necessitated close monitoring. Alongside the social and environmental impacts, the 28 May 2025 Blatten event also caused a significant economic impact, with initial estimated costs of around 320 million Swiss Francs (Islam et al., 2025).

3 Methods

3.1 Novel automated monitoring workflow

In this study we introduce a new automated, end-to-end workflow for multitemporal 3D monitoring of complex mountainous terrain, using an UAV operated from a dock. The workflow comprises five core components (Fig. 4): (a) flight planning, (b) flight management, execution, data capturing, and data upload done by the UAV dock, (c) image processing and dense 3D reconstruction, (d) spatiotemporal change and displacement analysis, and (e) accuracy assessment. The system is designed for near-continuous operation with minimal human intervention, enabling frequent and consistent surveys in complex and remote environments.

https://doi.org/10.5194/egusphere-2025-6432
Preprint. Discussion started: 4 January 2026

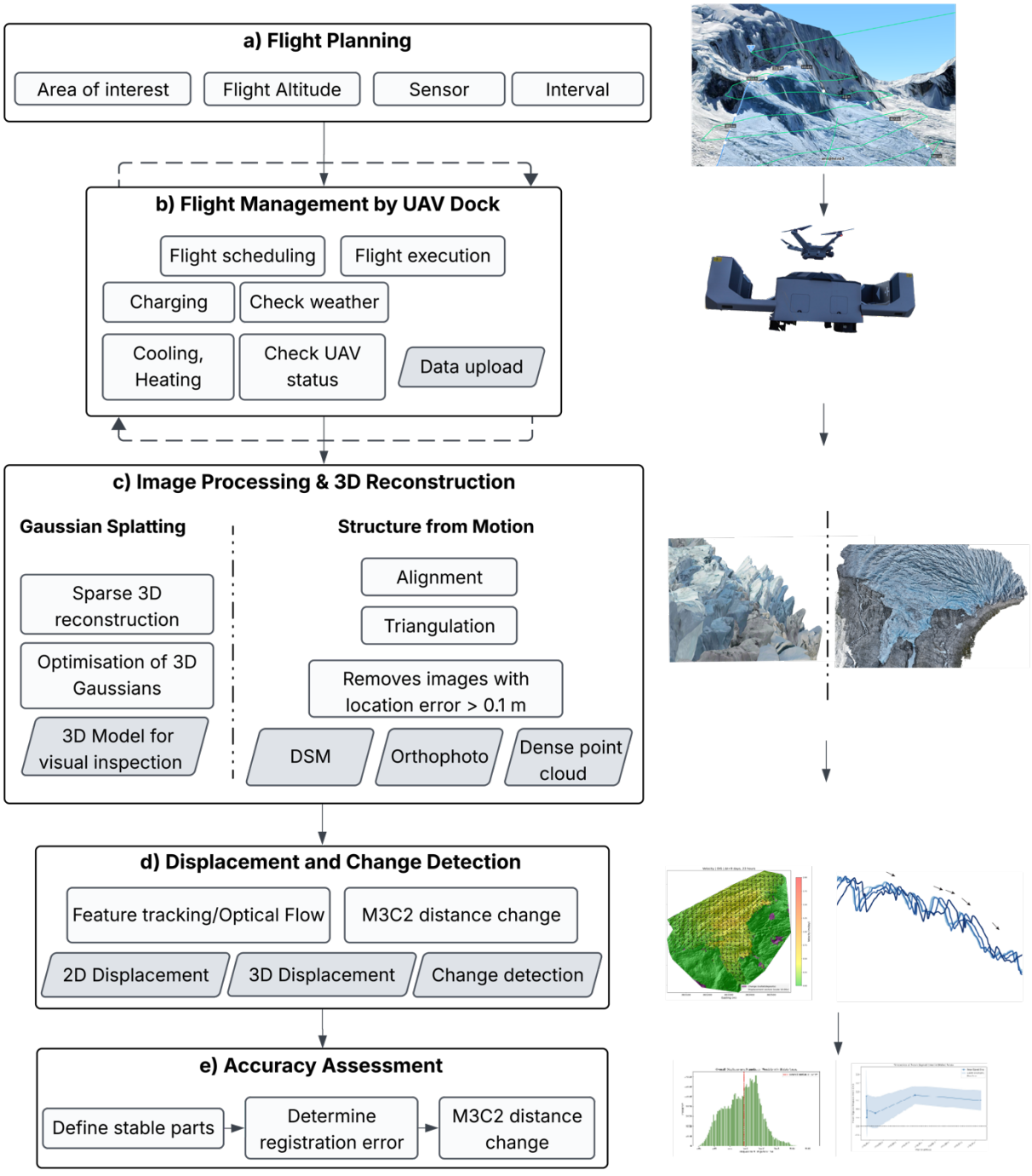

Figure 4 Workflow for multitemporal UAV monitoring and displacement and change detection analysis in alpine terrain, consisting of a) flight planning, b) flight management by the UAV dock, c) image processing and 3D reconstruction, d) spatiotemporal change and displacement detection, and e) accuracy assessment.

https://doi.org/10.5194/egusphere-2025-6432
Preprint. Discussion started: 4 January 2026

3.2 Data capturing using an automated UAV system

The automated UAV system consists of an UAV dock (in this study the DJI Dock 2 & 3) and its compatible multirotor UAVs Matrice 3D and 4D. The dock provides weatherproof housing, inductive battery charging, thermal regulation (cooling/heating), data transmission, and enables remote mission execution. The inbuilt weather station allows for wind speed and precipitation monitoring and prohibits the UAV to take off in case of bad weather. For terrain adaptive flight planning and the UAV and dock management, we used the cloud-based software DJI FlightHub 2 (FH2). The UAVs are equipped with a 20 Megapixel RGB sensor with a mechanical shutter. Detailed technical specifications of the camera sensor are presented in Table 1. For the geo-localisation, we use the inbuild RTK-GNSS and correction data from base stations nearby, streamed via NTRIP. For the tests in Norway, the system was not permanently installed; instead, we deployed the UAV dock temporarily at each site, with a pilot and observer present to ensure compliance with aviation safety regulations. Power was supplied by two 600 Wh portable power stations and communication with the dock was established using a local network, provided by a 4G router and connection via ethernet cable. Flight missions were scheduled at hourly, daily, and weekly intervals to capture high-resolution aerial imagery. Terrain-following flight paths were generated using a high-resolution digital elevation model (DEM) derived from the initial survey at each site. In the flight planning phase, the area of interest and the target ground sample distance (GSD) was manually selected. Redundant image coverage with at least 85% forward and lateral overlap was implemented to ensure robust 3D reconstruction under varying illumination and surface conditions. Table 2 shows an overview of the UAV operations at the different test sites. In Blatten, two UAV docks (DJI Dock 3) were installed close to the evacuation zone, and communication was established using a 4G router and a Starlink access point. Each flight at 150 m altitude captured imagery with 4.37 cm per pixel resolution, georeferenced using RTK and virtual ground control points.

Table 1 Technical specifications of the UAV camera sensors

Camera Model	Resolution	Focal Length	Pixel Size	Precalibrated	Min. Shooting Interval
M4D	5280 x 3956	12.29 mm	3.36 x 3.36 µm	Yes	0.5 s
M3D	5280 x 3956	12.29 mm	3.36 x 3.36 µm	Yes	0.7 s

https://doi.org/10.5194/egusphere-2025-6432
Preprint. Discussion started: 4 January 2026

Table 2 Overview of UAV operations at study sites

	Supphellebreen	**Skjøld**	**Blatten**
Dates	Sep-Nov 2024	Aug 24 - June 2025	May-November 2025
No. of Flights	17	7	55
Equipment	DJI Dock 2, Matrice M3D	DJI Dock 2, Matrice M3D	DJI Dock 2 & 3, Matrice M3D & M4D
Area of Interest	0.5 km²	1.02 km²	4.5 km²
Time to map the AOI	27 min	59 min (2 flights)	150 min (2 flights)
Flight Intervals	1h – 2 weeks	Daily – monthly	Daily – weekly
Mean No. of images per plight	1623	3112	2200
Mean GSD	1.89 cm pixel^{-1}	2.02 cm pixel^{-1}	4.37 cm pixel^{-1}
Mean Altitude	70 m	75 m	150 m
Estimated Surface Velocities	> 1 m day^{-1}	< 1 m year^{-1}	< 0.1 m day^{-1} (deposits)

3.3 Data processing workflow

3.3.1 From multi-view imagery to 3D: Gaussian Splatting and Structure from Motion processing

After mission completion, the acquired aerial imagery was transferred to the internal data storage of the dock and then uploaded to FH2 and stored for further analysis following our processing pipeline. For the dense 3D reconstruction, we implemented two distinct processing pathways (Fig. 5c): (1) a rapid 3D reconstruction approach based on Gaussian Splatting (Kerbl et al., 2023), which is capable of providing timely situational awareness for decision-makers, media, and the public, and (2) a photogrammetric Structure-from-Motion (SfM) pipeline aimed at producing high resolution point clouds, orthophotos, and digital surface models (DSMs). For the SfM 3D reconstructions we used DJI Terra (cloud processing implemented in Flighthub 2) and opendronemap (OpenDroneMap Authors ODM, 2020).

3.3.2 Change detection and displacement analysis

The photogrammetric products obtained from the SfM processing were further analysed to detect changes such as rockfalls or ice calving, 3D and 2D displacements. For three-dimensional displacement analysis, we applied the Multiscale Model-to-Model Cloud Comparison M3C2 algorithm (Lague et al., 2013) to the point clouds, enabling quantification of surface changes along the normal direction of the reference surface. For the multitemporal analysis, we used the py4dgeo library for change analysis in 4D (3D + time) point clouds (py4dgeo Development Core Team, 2022). For the calculation of two-dimensional horizontal displacements, we used multidirectional hillshades (generated from the DEMs) and applied the Dense Optical Flow algorithm Dense Inverse Search (DIS) (Kroeger et al., 2016). Previous studies have shown that DIS overcomes the limitations

https://doi.org/10.5194/egusphere-2025-6432
Preprint. Discussion started: 4 January 2026

of classical area-based algorithms, such as Phase Correlation (PC), which frequently suffer from decorrelation noise and restricted velocity ranges when analysing fast-moving glaciers and complex landslides (Hermle et al., 2022). DIS, an intensity-based approach (Kroeger et al., 2016) proved to be a more sensitive, less rigid, more flexible, and less constrained than traditional methods. DIS performed robustly under unfavourable illumination conditions and was capable of reliably tracking displacements in challenging steep high-alpine sites. Nevertheless, in areas where extremely rapid surface motion occurs, DIS tends to underestimate displacements, and the results obtained from such areas should therefore be interpreted with caution (Hermle et al., 2022).

3.3.3 Accuracy assessment

In order to support confidence in the obtained results, we hereby include an assessment of data accuracy and quality, although this is not the primary aim of this study. For the accuracy assessment, we used the dataset collected at Supphellebreen, as it represents the densest and most complete dataset among the three case studies. To assess the data quality and accuracy of the displacement measurements, we manually defined stable, non-moving reference areas ("stable areas") within the proximity of the glacier fronts, following common practice in UAV-based monitoring studies (e.g., Chudley et al., 2019). Due to inaccessibility and the risk of icefall and avalanches, ground control points could not be installed. We quantified the uncertainty of both 2D surface displacements (DIS optical flow) and 3D changes (M3C2) by measuring residuals in these areas. The variability of these residuals provides an empirical estimate of the detection limit at 95% confidence, expressed as $LoD_{95} = 1.96 \cdot \sigma$, where σ is the standard deviation of the residuals. As in previous studies (Fey & Wichmann, 2017; Kromer et al., 2017; Lague et al., 2013) we interpreted this 95% confidence interval or Level of Detection at 95% (LoD_{95}) as an estimate of the minimum detectable change.

4 Results

In the following section, we highlight representative results for each specific study site. The findings reveal that automated UAV systems can effectively monitor surface changes and velocity patterns with a high temporal and spatial resolution.

https://doi.org/10.5194/egusphere-2025-6432
Preprint. Discussion started: 4 January 2026

4.1 Monitoring of the icefall at Supphellebreen

The dataset collected at Supphellebreen offers unique insights on glacier dynamics, especially short-term processes, including acceleration phases of the glacier and single seracs (standing blocks of ice in the icefall), crevassing, and several dry calving events (Fig. 5). The glacier surface velocities at the icefall of Supphellebreen between September and November ranged from 0.4 to 1.5 m day^{-1}, with higher rates observed in steeper sections of the icefall (Fig. 5a-d). In the steepest areas with the highest

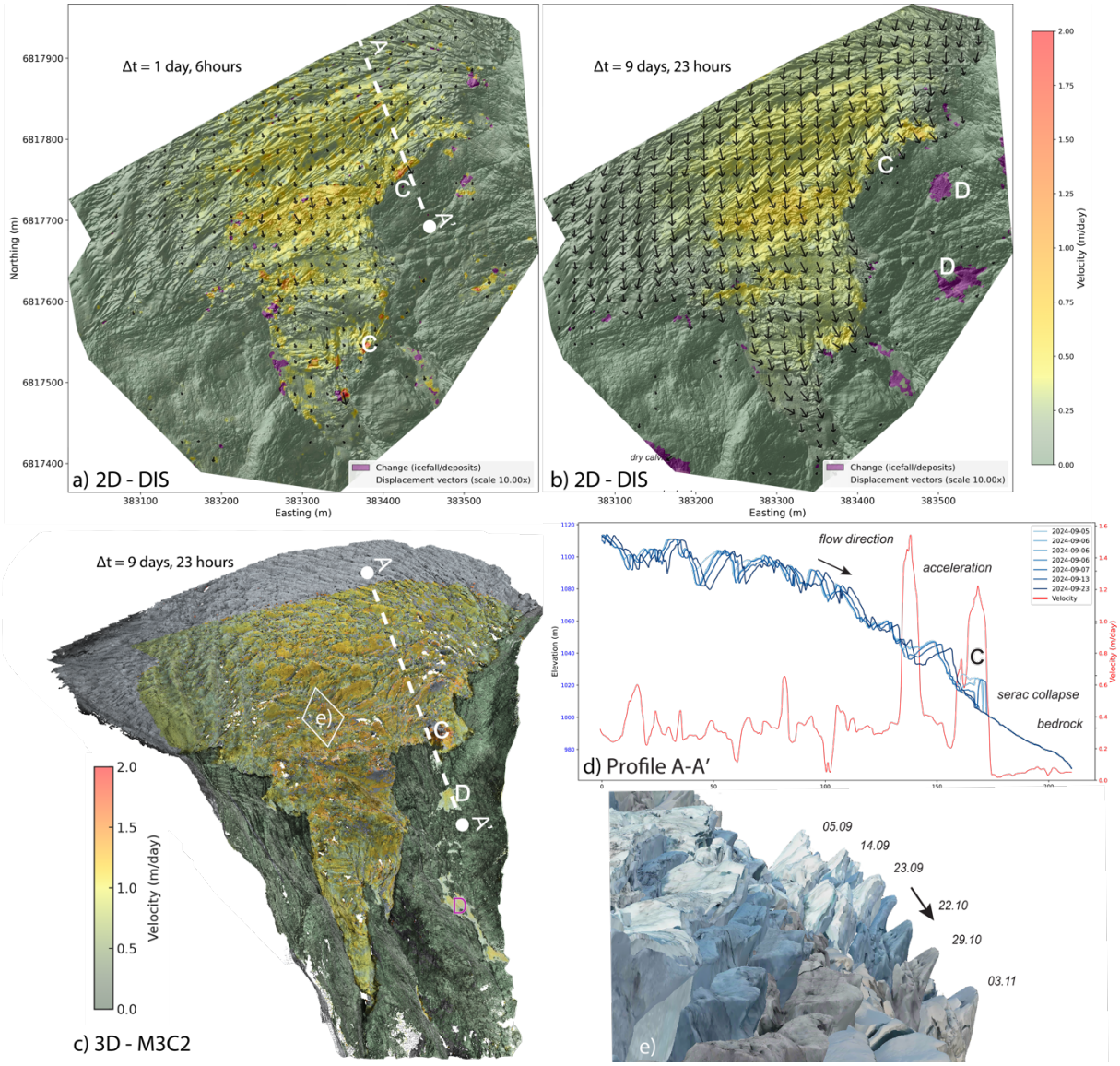

Figure 5 Changes detected at the upper part of Supphellebreen. a) Horizontal displacement (DIS) for a one-day interval, b) for a ten-days interval. c) 3D changes (M3C2) during the same time interval. d) Longitudinal profile A-A', showing glaciers surface and the flow direction between 5 and 23 September 2024. The red line shows the horizontal velocity along that profile. Point C marks a section that showed increased acceleration prior collapse. The deposits are marked with a D below in b). e) 3D models derived by Gaussian Splatting showing the glaciers surface change between 5 September and 3 November.

https://doi.org/10.5194/egusphere-2025-6432
Preprint. Discussion started: 4 January 2026

velocities, a maximum interval of about 10-15 days was possible, otherwise too high displacement rates led to decorrelation in the data. We could determine volumes and detect pre-failure acceleration of single seracs (Fig. 5a,d; marked with a C), exceeding 5 times the normal ice velocities. In the subsequent surveys, we identified run-out and ice deposition (marked with a D). Flow direction was mainly towards the southeast following the terrain, and there was minimal displacement towards the terminal moraine. Surface elevation changes in those almost stagnant ice zones indicated ablation rates of up to -0.06 m day^{-1}. Gaussian Splatting was used to create photorealistic 3D representations of the glacier surface from the different mapping campaigns (Fig. 5e).

https://doi.org/10.5194/egusphere-2025-6432
Preprint. Discussion started: 4 January 2026

4.2 Monitoring of a complex unstable rock slope at Skjøld

250 We demonstrated the system's ability to monitor and analyse the kinematics of the unstable rock slope at Skjøld (Fig. 6). Annual horizontal displacements at the site typically remain below 1 m and generally range between 0.2 and 0.4 m. The multitemporal photogrammetric data collected in this study allow us to delineate the extent of the instability (Fig. 6a,b) and to

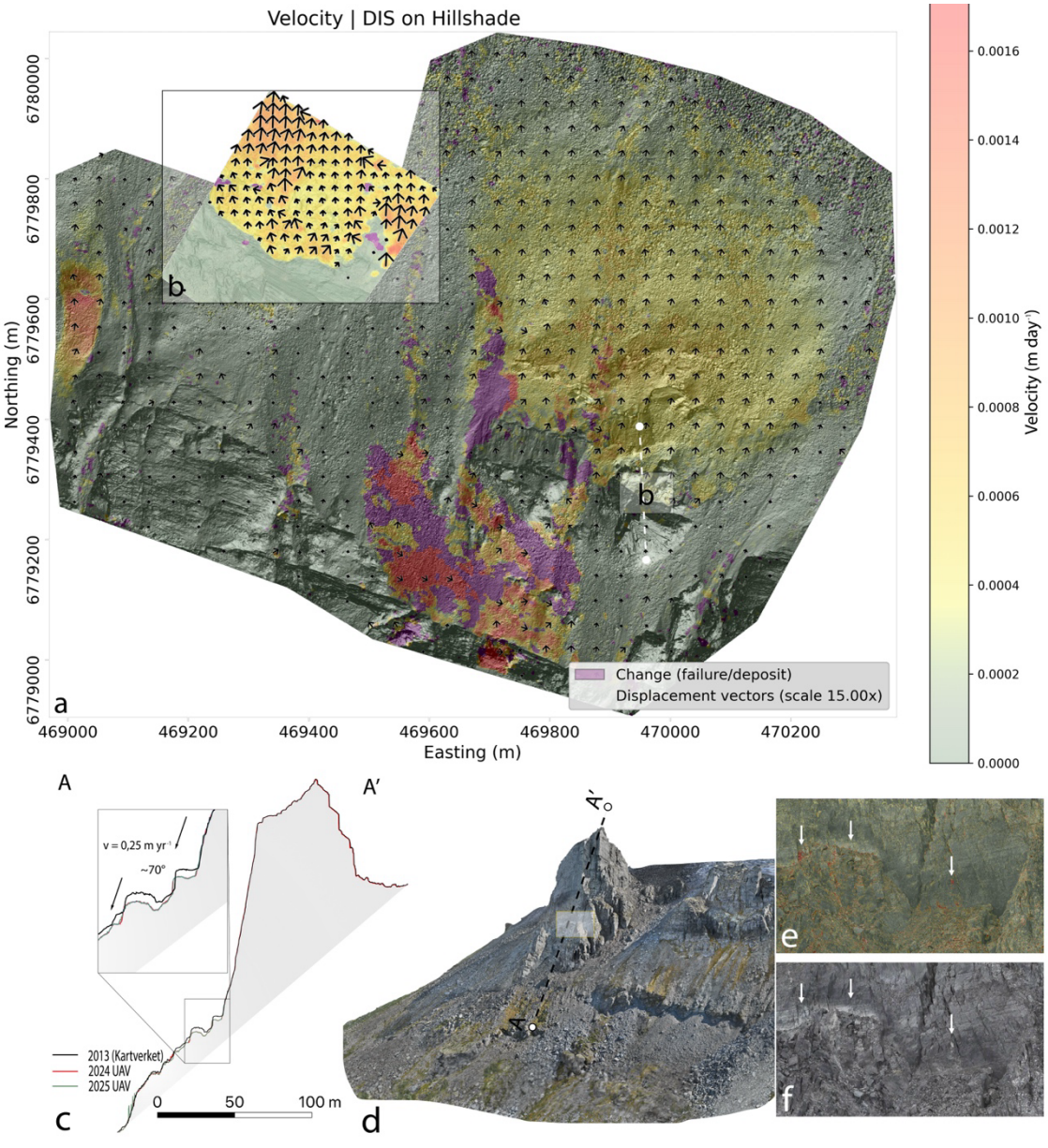

Figure 6 Monitoring results at the complex unstable rock slope Skjøld. a) 2D displacement field (DIS). b) Inset shows the contact between the "tower" and the area with higher displacement rates (purple shows changes, such as rockfall detachment and deposition). c) Profile showing the displacement vectors and the surface 2013, 2024, 2025. d) 3D model (Gaussian Splatting) showing the main section of the rock slope. e) DIS and f) Photograph showing the detachment of several rockfalls from the "tower" between August and November 2024.

https://doi.org/10.5194/egusphere-2025-6432
Preprint. Discussion started: 4 January 2026

assess the kinematic behaviour of individual structural features such as the isolated rock towers and the scree slope underneath (Fig. 6b,c). Most of the scree slope shows displacement rates of approximately 0.25 m yr^{-1}, while no measurable movement was detected in the rock towers. If the towers should move downslope, their displacement remains below the detection threshold of our displacement analysis. Short-term GB-InSAR campaigns by NVE confirm that most displacement is concentrated directly below the towers, which is consistent with the UAV-derived delineation of the instabilities (Fig. 6b,c). Using the point clouds and DEMs we could reconstruct the 3D displacement vector which dips approx. 70° towards the north. Consequently, the horizontal component represents only a small fraction of the total displacement. Between August and November 2024 several smaller rockfalls could be detected from the tower (Fig. 6d-f).

https://doi.org/10.5194/egusphere-2025-6432
Preprint. Discussion started: 4 January 2026

4.3 Post-disaster UAV mapping and rapid response at Blatten

The automated monitoring campaign following the rock-ice avalanche event at Blatten highlights the possibilities offered by
265 automated UAV systems in post-disaster response. Two DJI Dock 3 units conducted twice-daily automated flights in close

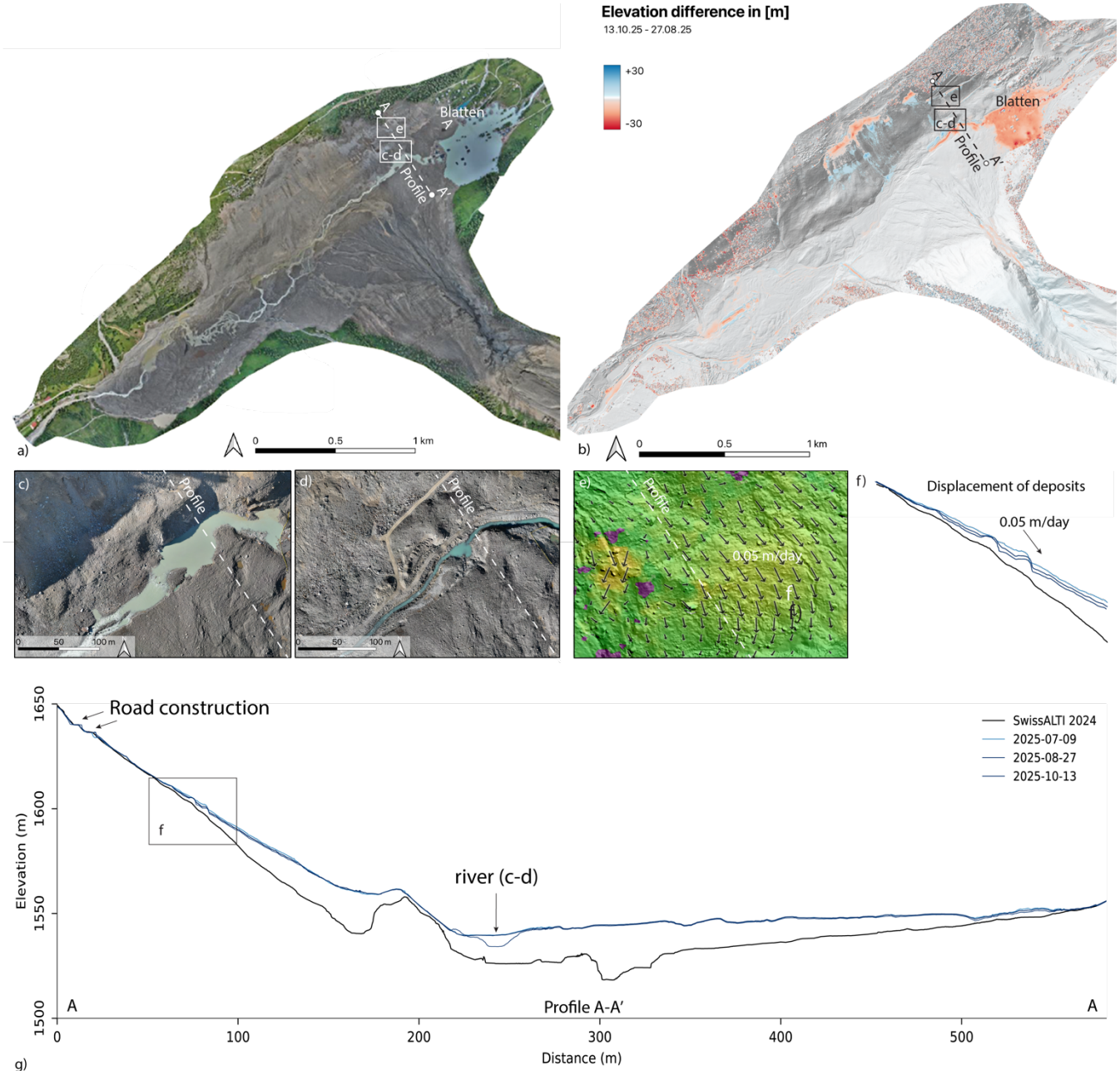

Figure 7 a) Orthophoto of the monitored area after the rock-ice avalanche event at Blatten. b) DoD elevation difference between 27 August and 13 October 2025. c-d) Changes along the river channel between 27 August and 13 October 2025. e) Horizontal displacement (DIS) of the deposits on the adjacent slope. f-g) Profiles through the deposits. The black lines correspond to the terrain before the event (Swiss Alti 2024), while the blue lines are selected UAV surveys after the event between July and October.

https://doi.org/10.5194/egusphere-2025-6432
Preprint. Discussion started: 4 January 2026

coordination with police and emergency authorities under SORA regulations. The docks were installed close to the evacuation zone and could only be visited once due to safety restrictions and ongoing hazard activity. This situation emphasises the critical importance of robust remote control and automated functionality for monitoring in hazardous, high-risk environments.

Figure 7 illustrates the monitored deposition area of the landslide (Fig. 7a) and representative analysis results, e.g., elevation differences between the two UAV campaigns from 27 August and 13 October 2025 (Fig. 7b), revealing zones of erosion (red), deposition (blue), and lake development, as well as subsequent lake outflow pathways (Fig. 7c,d). Due to the melting of ice-rich debris, subsidence and downslope displacement affect the deposits (Fig. 7e,f). The highest displacement rates were recorded in the run-up deposits on the SE-facing slope reaching 0.05 m day^{-1} between July and August, gradually decreasing over time. The cross-sections (Fig. 7g) compare pre-event topography (SwissALTI 2024) with three UAV-derived post-event mapping, and also depict recovery efforts, such as newly constructed access roads.

4.4 Accuracy assessment

The results of the camera location error analysis for the UAV surveys are summarized for each study site in Table 3. An accuracy assessment was conducted only for Supphellebreen using stable reference areas located on bedrock below the glacier front (Fig. 8a). The analysis of 2D displacement measurements derived from optical flow (DIS), yield a mean level of detection (LoD_{95}) of 0.092 m with min/max values ranging between 0.056 and 0.171 m (Fig. 8b). For the 3D displacement analysis based on point clouds and the M3C2 algorithm, the mean LoD_{95} across all surveys was 0.074 m, with values ranging from 0.041 to 0.091 m depending on the acquisition date. Temporal variability in LoD_{95} reflects differences in georeferencing quality between surveys (Fig. 8c,d). These results indicate that displacement signals exceeding the calculated LoD_{95} thresholds can be interpreted with high confidence as true surface change rather than noise. Importantly, LoD_{95} values should be determined for each survey pair and serve as a critical quality metric, establishing the threshold above which measured displacements can be regarded as reliable.

Table 3 Mean reprojection and georeferencing error for each study site

Study Site	Number of images	Reprojection error RMSE [px]	Georeferencing RMSE [m]	GSD [cm px^{-1}]	Average fligth altitude [m]	Aerotriangulation coverage area [km^2]
Supphellebreen	581	1.02	0.03	3.83	81	0.52
Skjøld	1244	1.03	0.08	4.19	100	1.31
Blatten	2248	-	0.03	4.37	150	4.5

https://doi.org/10.5194/egusphere-2025-6432
Preprint. Discussion started: 4 January 2026

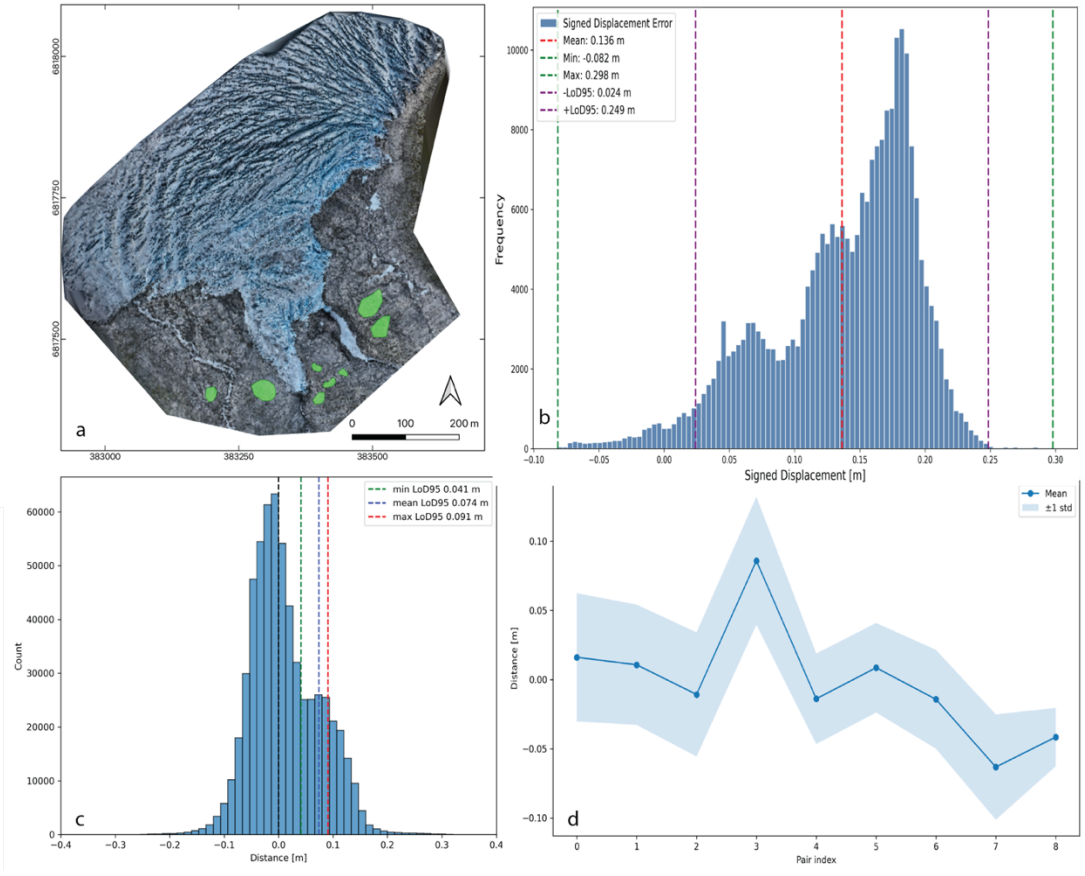

Figure 8 Accuracy assessment for the Supphellebreen site. a) Defined stable areas (bedrock) below the glacier front. b) Derived displacement in stable areas (DIS). c) M3C2 and the corresponding LoD values, and d) mean displacements and changes of the LoD over time for the different surveys.

Figure 9 shows a comparison of manually measured displacement vectors from the hillshade time series and DIS optical flow derived vectors. The agreement between the two datasets is strong ($R2$=0.798), indicating that the optical flow approach captures the main displacement signal reliably. The manual vectors were independently measured by two authors to reduce individual observer bias; however, a degree of subjectivity remains unavoidable. Manual vector estimation is inherently challenging, particularly in areas with low contrast or complex surface patterns, and small discrepancies in vector magnitude and orientation are therefore expected.

https://doi.org/10.5194/egusphere-2025-6432
Preprint. Discussion started: 4 January 2026

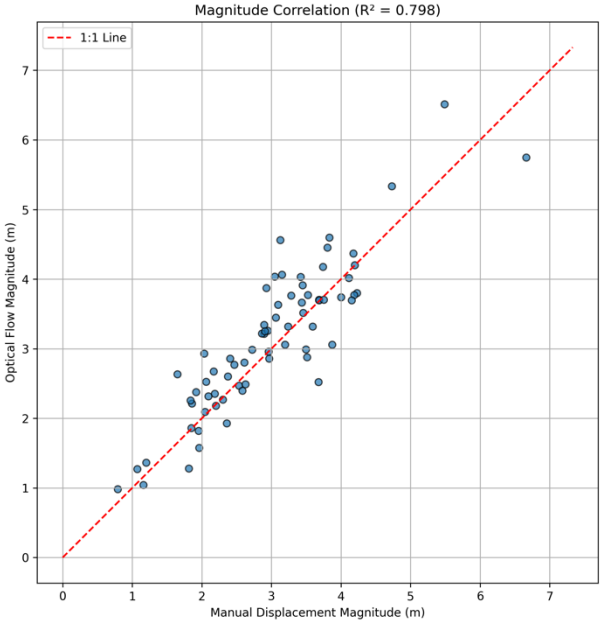

Metric	Manual	Optical Flow	Difference
Mean	2.98	3.13	0.16 (Bias)
Std Dev	1.02	1.05	0.48
Min	0.79	0.98	-1.15
Max	6.66	6.51	1.44

Figure 9 Comparison between manuel derived displacement vectors and the DIS optical flow results (on hillshades)

5 Discussion

Automated UAV systems offer a paradigm shift in the monitoring of dynamic geohazard environments. This study demonstrates, for the first time that UAV docks can support fully automated, high-frequency observations of unstable slopes, glacier hazards and a post-disaster landscape. By transitioning from campaign-based surveys to a continuous near-real-time monitoring approach, rapid surface changes that would otherwise go undetected can be captured. UAV docks placed at high-risk sites can enable more frequent repeated missions, needed for situational awareness in critical phases of hazard evolution, without exposing personnel to risk. Systematic and automated processing of the resulting image series yields centimetre-level displacement fields that resolve subtle deformation and changes in displacement rates. Detecting acceleration in displacement is crucial for timely decision making in settings where slope failures threaten communities or infrastructure, and rapid actions may be required.

5.1 Analytical capabilities and temporal resolution

Recent advances in computer vision, image-based processing, and point-cloud algorithms have considerably expanded UAV monitoring capabilities. Modern change detection methods such as image correlation, optical flow, and feature-based tracking achieve sub-pixel precision (Hermle et al., 2022; Xiao et al., 2023). Deep learning-based image matching has further improved robustness and accuracy, outperforming conventional cross-correlation or feature-tracking approaches in glacier surface

https://doi.org/10.5194/egusphere-2025-6432
Preprint. Discussion started: 4 January 2026

velocity estimation (Zandler et al., 2025). For three-dimensional datasets, the Multiscale Model-to-Model Cloud Comparison (M3C2) algorithm (Lague et al., 2013) remains the benchmark for point-cloud change detection. Today, a steadily growing diverse suite of algorithms with variable sensitivity, computational demand, and spatial resolution enables tailored analyses.

Accuracy represents a core issue of reliable monitoring solutions. Current RTK positioning allows centimetre-scale georeferencing, which is generally sufficient for detailed geomorphic mapping and hazard-monitoring applications. For slowly deforming slopes (<5 cm yr^{-1}), however, detection remains challenging; nevertheless, repeated imaging provides valuable insights into near-surface processes such as rockfall activity and when equipped with infrared sensors also waterflows, air flows and temperature fields. At Skjøld, slope deformation within a two-week time interval could not be estimated due to the low displacement rates, yet frequent surveys identified detachment zones of individual rockfalls.

Maintaining consistent flight geometry (e.g., area to cover and flight trajectories), integrating PPK or GCP corrections, and applying co-registration techniques such as for example ICP (Besl & McKay, 1992) or xDEM (xDEM contributors, 2023) can contribute to reducing systematic errors and lower the LoD_{95} to below 0.5×GSD. In our study, network RTK via CORS with 20–30 km baselines yield acceptable accuracy (<5-10 cm), though shorter baselines or local base stations could further improve results. While we intentionally varied flight plans to test different configurations, future deployments should emphasize consistent trajectories and incorporate co-registration algorithms. In optimal conditions, LoD_{95} values can improve from 1×GSD to approximately 0.3–0.5×GSD (James et al., 2017; Santise et al., 2014). When lower thresholds are needed, reducing the flight altitude, or establishing local correction networks can further enhance precision (McMahon et al., 2021).

The dynamic nature of geohazards, such as landslides and glacier collapses that can further develop into multi-hazard cascades, highlights the need for rapidly deployable and adaptive monitoring technologies. The flexibility of automated UAV systems allows adaptive scheduling from weekly missions for slow-moving or creeping slopes to sub-daily operations during critical phases. Following catastrophic events, UAV docks can provide near-real time situational awareness, supporting rapid topographic mapping for search, rescue and damage assessment, as documented in the case of Blatten.

In rapidly changing environments, a high temporal data resolution is essential. For instance, at Supphellebreen, long flight intervals exceeding ten days led to feature mismatches and reduced tracking accuracy, whereas more frequently collected UAV time series captured accelerated ice velocities and serac collapses, demonstrating that high-frequency imagery is crucial for accurate risk assessment. High-resolution terrain data further allow precise displacement and volume calculations, which are essential for run out modelling, the identification of controlling factors, post event analysis and support for mitigation planning.

High-resolution, high-frequency UAV data bridge the observational gap between coarse-resolution satellite imagery (e.g., Sentinel, Landsat, Planet) and sporadic UAV campaigns. The resulting 4D datasets offer a robust foundation for training deep learning models (e.g., Ma & Mei, 2021) and improving our understanding of slope and glacier dynamics. Unlike one-dimensional line of sight measurements, UAV photogrammetry enables the derivation of full 3D displacement vectors. UAVs can also integrate multispectral, thermal, or lightweight meteorological sensors (e.g., Haualand et al., 2025), providing valuable environmental parameters directly at the site. Recent advances in computational efficiency and automated pipelines have made near-real-time analysis feasible, enabling responsive and data-driven hazard monitoring (Kothari & Momayez, 2018).

https://doi.org/10.5194/egusphere-2025-6432
Preprint. Discussion started: 4 January 2026

A challenge in UAV-based monitoring relying on optical imagery is the influence of weather and illumination conditions. Weather conditions such as fog, heavy winds or intense precipitation may hinder take-offs and restrict flight frequencies, and varying illumination conditions can adversely affect image alignment, surface reconstruction, and subsequent change detection. Variations in sunlight intensity, shadow extent, and surface reflectance often lead to radiometric inconsistencies between image sets, particularly in complex alpine terrain. At Supphellebreen, most automated UAV flights were conducted during civil twilight (approximately ten minutes after sunset), providing diffuse, uniform illumination and minimal shadowing, conditions that improve reconstruction and displacement analysis consistency. However, such survey scheduling is not always feasible due to operational or weather-related constraints. Advancements in illumination normalization, shadow-compensation algorithms, and the use of radiometrically invariant image features will therefore be crucial to improve the reliability and comparability of optical UAV-based monitoring across variable environmental conditions (e.g., Shen et al., 2025). Especially at the sites in Norway, we noted that precipitation and low fog can often hinder remote sensing such as satellite image acquisition or fixed terrestrial camera observations. Automated UAVs can either fly above the cloud barrier, or low enough, providing crucial observations when other sensors fail. Nevertheless, we suggest using complementary and redundant instrumentation in critical situations at high-risk sites (e.g., Choi et al., 2024; Maschler et al., 2025).

During our deployments, automated missions operated successfully under light rain and snowfall, though image quality was occasionally degraded by lens droplets. Modern weather resistant docks and waterproof UAVs equipped with environmental control and real-time weather monitoring mitigate many of these issues, yet rapidly changing conditions near glaciers or steep slopes can still necessitate mission aborts for safety. The combination of high-altitude overview missions at around 100 m and up to max.120 m above ground combined with low-altitude detailed surveys at 20-50 m above ground enable scalable and flexible monitoring.

5.2 Perspectives on scalable deployment and early warning systems

Effective hazard communication and vulnerability reduction depend on providing clear and understandable information to populations at risk (World Meteorological Organization, 2022). Our results show that automated UAV systems for geohazard monitoring can supply authorities with actionable technical data before, during, and after disasters, while also generating accessible visual insights (e.g. 3D models & the Gaussian Splatting outputs) that can strengthen situational awareness. A single strategically positioned UAV dock can be used to monitor multiple hazards such as rockfalls, icefalls, and glacier lakes while simultaneously serving as a simple meteorological station, thus collecting information that serves civil protection. Although the initial investment in automated UAV systems is relatively high, especially when advanced equipment such as LiDAR and thermal sensors are included, compared to the logistics and personnel costs of traditional surveys the recurring costs per inspection or monitoring interval decrease sharply after deployment.

Beyond environmental constraints, regulatory frameworks currently represent one of the main barriers to operational scaling. Automated flights beyond visual line of sight (BVLOS) often require special permissions, airspace coordination, and risk mitigation measures (e.g., parachutes, geofencing). The harmonization of such frameworks across jurisdictions will be critical

https://doi.org/10.5194/egusphere-2025-6432
Preprint. Discussion started: 4 January 2026

for widespread adoption of automated UAV networks. Furthermore, setting priorities for geohazard monitoring and technology deployment remains challenging for vulnerable regions with a high density of potentially hazardous sites and limited financial resources (Ghosh, 2025; Huggel et al., 2020). Additionally, in regions where mountains hold cultural or spiritual significance, social acceptance becomes a decisive factor in the implementation of UAV monitoring technology, and its long-term sustainability (Fraser, 2017). Participatory approaches, involving close dialogue and collaboration between scientists, authorities and the local community, could enable the co-development of robust and adaptive monitoring frameworks that integrate local knowledge systems (e.g., Fan et al., 2025; Hermans et al., 2022). Broader adoption depends on development of appropriate legal frameworks, equitable access to technological infrastructure, the availability of skilled personnel and social acceptance (du Plessis & Amoah, 2025; Islam et al., 2025). We recommend that future research focuses on integrating near-continuous UAV data into existing early warning systems. Moreover, we would like to emphasise that technological innovations in risk monitoring and visualisation need to be complemented by participatory educational initiatives and strategic capacity building programs to effectively increase risk awareness among citizens and support community resilience.

5.3 Rapid response UAV dock operations: Lessons from Blatten

The 28 May 2025 Blatten landslide in Switzerland highlights both the potential and complexity of using automated UAV dock systems for rapid crisis response. Following the catastrophic failure event, the dock system facilitated remote access and provided a flexible method for data acquisition under restricted conditions. While the UAV system demonstrated high reliability, operational success depended on expert oversight and pre-established coordination protocols. Operating across elevations from 1500 to 3000 m in changing alpine meteorology required precise remote supervision and dynamic mission adjustment. Airspace management was a major constraint for entirely automated operation, as BVLOS operations in zones with dense helicopter activity after the event demanded real-time air traffic monitoring using tools. In Blatten, Skylens was used, a proprietary airspace monitoring system developed by RemoteVision in collaboration with FLARM (flarm.com). It integrates position messages from multiple aviation separation and traffic awareness technologies (e.g., FLARM, ADS-B and related systems), which are fused and visualised in real time on a unified map interface. This interface provides a comprehensive overview of surrounding air traffic and was actively used by the dock operator to monitor helicopter and aircraft traffic in the vicinity of the monitoring area, thereby supporting safe BVLOS operations in the dynamically changing post-event airspace. Achieving photogrammetric accuracies of ±5 cm over 4.5 km² required careful optimization of flight parameters and image density to balance precision and data volume (~10 GB per flight). These findings underscore that successful rapid-response mapping depends not only on robust technology but also on proactive system preparation, inter-agency coordination, and skilled human oversight capable of operating within complex environmental and regulatory frameworks.

https://doi.org/10.5194/egusphere-2025-6432
Preprint. Discussion started: 4 January 2026

6 Conclusions

This study demonstrates that automated UAV systems can substantially improve the monitoring of glacier and rock slope instabilities in remote alpine terrain. Across three different test sites, the application of automated UAVs coupled with subsequent automated image processing and integrated displacement and change detection enabled safe and high-frequency data acquisition at centimetre-level accuracy. Automatically collected UAV data with high spatio-temporal resolution bridge the observational gap between satellite imagery and sporadic, manual UAV campaigns. Near-continuous UAV observations revealed short-term dynamic processes such as serac acceleration, scree slope creep, and post-failure terrain subsidence. These findings highlight the value of automated UAVs for both monitoring and post-disaster assessment, particularly where rapid hazard evolution requires flexibility and adaptability to gain situational awareness. However, favourable regulatory conditions, reliable power and communication infrastructure, and local expertise remain essential preconditions for scalable deployment. Overall, UAV dock-based monitoring represents a promising step toward automated hazard monitoring networks in a large variety of geo-hazardous environments, with the potential to enhance risk mitigation and strengthen the resilience of exposed communities. Future research should focus on integrating these systems into fully operational early warning frameworks.

Acknowledgements

The study at Supphellebreen was conducted within the framework of the JOSTICE project, funded by the Research Council of Norway (RCN grant no. 302458). We acknowledge DJI and Boston, in particular Kjetil Hatlen for providing access to a demonstration unit of the UAV drone dock and for technical assistance. For the Blatten case study, we acknowledge Terradata (Switzerland), in particular Alain Oggier for his role as the local surveying technician. We further acknowledge the Dienststelle Naturgefahren Wallis (Canton of Valais) including the cantonal geological service for institutional support and coordination in the context of natural hazard monitoring. We acknowledge the use of AI tools for coding assistance.

Code and data availability

The code, data and supplementary animations will be available on DataverseNO at a later stage.

Author contributions

AM: Conceptualization, Data collection & curation, Analysis, Methodology, Validation, Visualization, Writing - original draft, review, and editing. **SL:** Conceptualization, Data collection, Analysis, Methodology, Validation, Visualization, Writing original draft, review, and editing. **LS:** Data collection, Writing - review and editing. **TS:** Conceptualization, Supervision, Writing - review and editing. **PS:** Conceptualization, Supervision, Writing - review and editing. **JCY:** Conceptualization, Supervision, Writing - review and editing. **HZ:** Writing - review and editing, Validation **US:** Data collection, Writing - review and editing.

https://doi.org/10.5194/egusphere-2025-6432
Preprint. Discussion started: 4 January 2026

Competing interests

Ueli Sager is CEO of the company Remote Vision, which is developer of Skylens in collaboration with the company FLARM

References

Åkesson, H., Sjursen, K. H., Schuler, T.V., Dunse, T., Andreassen, L. M., Gillespie, M.K., Robson, B. A., Schellenberger, T., & Yde, J.C. (2025). Recent history and future demise of Jostedalsbreen, the largest ice cap in mainland Europe. *The Cryosphere*, *19*(11), 5871–5902. https://doi.org/10.5194/tc-19-5871-2025

Besl, P. J., & McKay, N. D. (1992). A Method for Registration of 3-D Shapes. *IEEE Transactions on Pattern Analysis and Machine Intelligence*, *14*(2), 239–256. https://doi.org/10.1109/34.121791

Büntgen, U., Oppenheimer, C., Farinotti, D., Nahtz, T., & Esper, J. (2025). The 2025 Blatten disaster in the Swiss Alps followed exceptional warming and highlights the vulnerability of people and heritage in glaciated landscapes. *Communications Earth & Environment 2025 6:1*, *6*(1), 994-. https://doi.org/10.1038/S43247-025-02994-8

Carrivick, J. L., Andreassen, L. M., Nesje, A., & Yde, J. C. (2022). A reconstruction of Jostedalsbreen during the Little Ice Age and geometric changes to outlet glaciers since then. *Quaternary Science Reviews*, *284*, 107501. https://doi.org/10.1016/j.quascirev.2022.107501

Choi, S.-K., Ramirez, R. A., Lim, H.-H., & Kwon, T.-H. (2024). Multi-source remote sensing-based landslide investigation: the case of the August 7, 2020, Gokseong landslide in South Korea. *Scientific Reports*, *14*(1), 12048. https://doi.org/10.1038/s41598-024-59008-4

Chudley, T. R., Christoffersen, P., Doyle, S. H., Abellan, A., & Snooke, N. (2019). High-accuracy UAV photogrammetry of ice sheet dynamics with no ground control. *Cryosphere*, *13*(3), 955–968. https://doi.org/10.5194/TC-13-955-2019

Clague, J. J., Huggel, C., Korup, O., & McGuire, B. (2012). Climate change and hazardous processes in high mountains. *Revista de La Asociacion Geologica Argentina*, *69*(3). https://doi.org/10.5167/uzh-77920

du Plessis, J., & Amoah, C. (2025). Factors hindering the use of unmanned aerial vehicles for construction project monitoring. *Discover Applied Sciences 2025 7:7*, *7*(7), 782-. https://doi.org/10.1007/S42452-025-07414-2

Dwivedi, R., Narayan, A. B., Tiwari, A., Dikshit, O., Singh, A. K., (2016). Multi-Temporal SAR Interferometry for Landslide Monitoring. *The International Archives of the Photogrammetry, Remote Sensing and Spatial Information Sciences*, *XLI-B8*, 55–58. https://doi.org/10.5194/ISPRS-ARCHIVES-XLI-B8-55-2016

Farinotti, D., Huss, M., Mylène Jacquemart, Mauro Werder, Jane Walden, Reto Knutti, Sonia Seneviratne, Olivier Gagliardini, Thomas Schuler, Erich Fischer, & David Bresch. (2025). *Birchgletscher Fact Sheet*. *88028-VAW-2025–06d*.

https://doi.org/10.5194/egusphere-2025-6432
Preprint. Discussion started: 4 January 2026

Fey, C., & Wichmann, V. (2017). Long-range terrestrial laser scanning for geomorphological change detection in alpine terrain – handling uncertainties. *Earth Surface Processes and Landforms*, *42*(5), 789–802. https://doi.org/10.1002/ESP.4022

Fraser, B. (2017, April). Learning from flood-alarm system's fate. *EcoAméricas*. https://cooperacionsuiza.pe/wp-content/uploads/2017/05/fraser_sat_carhuaz_ecoamericas17.pdf

Frodella, W., Salvatici, T., Pazzi, V., Morelli, S., & Fanti, R. (2017). Gb-InSAR monitoring of slope deformations in a mountainous area affected by debris flow events. *Natural Hazards and Earth System Sciences*, *17*(10), 1779–1793. https://doi.org/10.5194/NHESS-17-1779-2017

Gerstner, R., Maschler, A., Schneider-Muntau, B., Agliardi, F., Avian, M., Frießenbichler, M., & Zangerl, C. (2025). The critical role of fracture propagation in the evolution of extensive, structurally preconditioned rockslides. *Engineering Geology*, *358*, 108359. https://doi.org/10.1016/J.ENGGEO.2025.108359

Ghosh, S. (2025). Living on the Edge of Fragile Majesty: An Introductory Note on Emerging Risks, Hazards and Disasters in the Himalaya. In S. Ghosh (Ed.), *The Himalaya Dilemma: Navigating Risk, Vulnerability, and Resilience in Geohazard-Prone Regions* (pp. 1–42). Springer Nature Switzerland. https://doi.org/10.1007/978-3-031-95083-4_1

Gillespie, M. K., Andreassen, L. M., Huss, M., de Villiers, S., Sjursen, K. H., Aasen, J., Bakke, J., Cederstrøm, J. M., Elvehøy, H., Kjøllmoen, B., Loe, E., Meland, M., Melvold, K., Nerhus, S. D., Røthe, T. O., Støren, E. W. N., Øst, K., & Yde, J. C. (2024). Ice thickness and bed topography of Jostedalsbreen ice cap, Norway. *Earth System Science Data*, *16*(12), 5799–5825. https://doi.org/10.5194/essd-16-5799-2024

Haualand, K. F., Sauter, T., Abermann, J., de Villiers, S. D., Georgi, A., Goger, B., Dawson, I., Nerhus, S. D., Robson, B. A., Sjursen, K. H., Thomas, D. J., Thomaser, M., & Yde, J. C. (2025). Meteorological Impact of Glacier Retreat and Proglacial Lake Temperature in Western Norway. *Journal of Geophysical Research: Atmospheres*, *130*(13). https://doi.org/10.1029/2024JD042715

Hermans, T. D. G., Šakić Trogrlić, R., van den Homberg, M. J. C., Bailon, H., Sarku, R., & Mosurska, A. (2022). Exploring the integration of local and scientific knowledge in early warning systems for disaster risk reduction: a review. *Natural Hazards 2022 114:2*, *114*(2), 1125–1152. https://doi.org/10.1007/S11069-022-05468-8

Hermle, D., Gaeta, M., Krautblatter, M., Mazzanti, P., & Keuschnig, M. (2022). Performance Testing of Optical Flow Time Series Analyses Based on a Fast, High-Alpine Landslide. *Remote Sensing*, *14*(3). https://doi.org/10.3390/rs14030455

Huang, G., Du, S., & Wang, D. (2023). Open Access Satellite Navigation GNSS techniques for real-time monitoring of landslides: a review. *Satellite Navigation*, *4*, 5. https://doi.org/10.1186/s43020-023-00095-5

Huggel, C., Carey, M., Emmer, A., Frey, H., Walker-Crawford, N., & Wallimann-Helmer, I. (2020). Anthropogenic climate change and glacier lake outburst flood risk: Local and global drivers and responsibilities for the case of lake Palcacocha, Peru. *Natural Hazards and Earth System Sciences*, *20*(8), 2175–2193. https://doi.org/10.5194/NHESS-20-2175-2020

https://doi.org/10.5194/egusphere-2025-6432
Preprint. Discussion started: 4 January 2026

Islam, N., Carrivick, J. L., Coulthard, T., Westoby, M., Dunning, S., & Gindraux, S. (2025). A growing threat of multi-hazard cascades highlighted by the Birch Glacier collapse and Blatten landslide in the Swiss Alps. *Geology Today*, *41*(5), 200–205. https://doi.org/10.1111/GTO.12526

James, M. R., Robson, S., d'Oleire-Oltmanns, S., & Niethammer, U. (2017). Optimising UAV topographic surveys processed with structure-from-motion: Ground control quality, quantity and bundle adjustment. *Geomorphology*, *280*, 51–66. https://doi.org/10.1016/j.geomorph.2016.11.021

Kerbl, B., Kopanas, G., Leimkuehler, T., & Drettakis, G. (2023). 3D Gaussian Splatting for Real-Time Radiance Field Rendering. *ACM Transactions on Graphics*, *42*(4), 14. https://doi.org/10.1145/3592433

Klimeš, J., Novotný, J., Rapre, A. C., Balek, J., Zahradníček, P., Strozzi, T., Sana, H., Frey, H., René, M., Štěpánek, P., Meitner, J., & Junghardt, J. (2021). Paraglacial Rock Slope Stability Under Changing Environmental Conditions, Safuna Lakes, Cordillera Blanca Peru. *Frontiers in Earth Science*, *9*. https://doi.org/10.3389/feart.2021.607277

Kothari, U. C., & Momayez, M. (2018). Machine Learning: A Novel Approach to Predicting Slope Instabilities. *International Journal of Geophysics*, *2018*, 1–9. https://doi.org/10.1155/2018/4861254

Kristensen, L., Czekirda, J., Penna, I., Etzelmüller, B., Nicolet, P., Pullarello, J. S., Blikra, L. H., Skrede, I., Oldani, S., & Abellan, A. (2021). Movements, failure and climatic control of the Veslemannen rockslide, Western Norway. *Landslides*, *18*(6), 1963–1980. https://doi.org/10.1007/s10346-020-01609-x

Kroeger, T., Timofte, R., Dai, D., & Gool, L. Van. (2016). *Fast Optical Flow using Dense Inverse Search*.

Kromer, R. A., Abellán, A., Hutchinson, D. J., Lato, M., Chanut, M.-A., Dubois, L., & Jaboyedoff, M. (2017). Automated terrestrial laser scanning with near-real-time change detection-monitoring of the Séchilienne landslide. *Earth Surf. Dynam*, *5*, 293–310. https://doi.org/10.5194/esurf-5-293-2017

Lague, D., Brodu, N., & Leroux, J. (2013). Accurate 3D comparison of complex topography with terrestrial laser scanner: Application to the Rangitikei canyon (N-Z). *ISPRS Journal of Photogrammetry and Remote Sensing*, *82*, 10–26. https://doi.org/10.1016/J.ISPRSJPRS.2013.04.009

Lelli, F., Mulas, M., Critelli, V., Fabbiani, C., Tondo, M., Aleotti, M., & Corsini, A. (2025). Leveraging High-Frequency UAV–LiDAR Surveys to Monitor Earthflow Dynamics—The Baldiola Landslide Case Study. *Remote Sensing 2025, Vol. 17, Page 2657*, *17*(15), 2657. https://doi.org/10.3390/RS17152657

Ma, Z., & Mei, G. (2021). Deep learning for geological hazards analysis: Data, models, applications, and opportunities. *Earth-Science Reviews*, *223*, 103858. https://doi.org/10.1016/J.EARSCIREV.2021.103858

Maschler, A., Snook, P., Schild, L., Samnøy, S. F., Kristensen, L., Dahle, H., Aalbu, J. H., Henriksen, H., Nerhus, S. D., & Scheiber, T. (2025). Multistage 54,000 m3 rockfall (Stampa, Western Norway): Insights from comprehensive monitoring and failure analysis. *Landslides*. https://doi.org/10.1007/s10346-025-02620-w

https://doi.org/10.5194/egusphere-2025-6432
Preprint. Discussion started: 4 January 2026

McMahon, C., Mora, O. E., & Starek, M. J. (2021). Evaluating the Performance of sUAS Photogrammetry with PPK Positioning for Infrastructure Mapping. *Drones*, *5*(2), 50. https://doi.org/10.3390/drones5020050

OpenDroneMap Authors ODM. (2020). *A command line toolkit to generate maps, point clouds, 3D models and DEMs from drone, balloon or kite images.* https://github.com/OpenDroneMap/ODM.

Picarelli, L., Lacasse, S., & Ho, K. K. S. (2021). *The Impact of Climate Change on Landslide Hazard and Risk* (pp. 131–141). https://doi.org/10.1007/978-3-030-60196-6_6

py4dgeo Development Core Team. (2022). *py4dgeo: library for change analysis in 4D point clouds*. https://github.com/3dgeo-heidelberg/py4dgeo

Rodriguez, J., Macciotta, R., Hendry, M. T., Roustaei, M., Gräpel, C., & Skirrow, R. (2020). UAVs for monitoring, investigation, and mitigation design of a rock slope with multiple failure mechanisms—a case study. *Landslides*, *17*(9). https://doi.org/10.1007/s10346-020-01416-4

Santise, M., Fornari, M., Forlani, G., & Roncella, R. (2014). Evaluation of DEM generation accuracy from UAS imagery. *The International Archives of the Photogrammetry, Remote Sensing and Spatial Information Sciences*, *XL–5*, 529–536. https://doi.org/10.5194/isprsarchives-XL-5-529-2014

Schlögl, M., Gutjahr, K., & Fuchs, S. (2022). *The challenge to use multi-temporal InSAR for landslide early warning*. *112*, 2913–2919. https://doi.org/10.1007/s11069-022-05289-9

Shen, X., Cao, Y., Sui, B., Zhang, S., & Feng, D. (2025). An automatic remote sensing image shadow compensation method utilizing reflectance differences and transfer learning. *GIScience and Remote Sensing*, *62*(1). https://doi.org/10.1080/15481603.2025.2487334

Stähli, M., Sättele, M., Huggel, C., McArdell, B. W., Lehmann, P., Van Herwijnen, A., Berne, A., Schleiss, M., Ferrari, A., Kos, A., Or, D., & Springman, S. M. (2015). Monitoring and prediction in early warning systems for rapid mass movements. *Natural Hazards and Earth System Sciences*, *15*(4), 905–917. https://doi.org/10.5194/nhess-15-905-2015

Stoffel, M., Trappmann, D. G., Coullie, M. I., Ballesteros Cánovas, J. A., & Corona, C. (2024). Rockfall from an increasingly unstable mountain slope driven by climate warming. *Nature Geoscience 2024 17:3*, *17*(3), 249–254. https://doi.org/10.1038/s41561-024-01390-9

Stuart-Smith, R. F., Roe, G. H., Li, S., & Allen, M. R. (2021). Increased outburst flood hazard from Lake Palcacocha due to human-induced glacier retreat. *Nature Geoscience 2021 14:2*, *14*(2), 85–90. https://doi.org/10.1038/s41561-021-00686-4

Walter, F., Hodel, E., Mannerfelt, E. S., Cook, K., Dietze, M., Estermann, L., Wenner, M., Farinotti, D., Fengler, M., Hammerschmidt, L., Hänsli, F., Hirschberg, J., Mcardell, B., & Molnar, P. (2022). Brief communication: An autonomous UAV for catchment-wide monitoring of a debris flow torrent. *Natural Hazards and Earth System Sciences*, *22*(12), 4011–4018. https://doi.org/10.5194/NHESS-22-4011-2022

https://doi.org/10.5194/egusphere-2025-6432
Preprint. Discussion started: 4 January 2026

World Meteorological Organization. (2022). *Early warnings for all: The UN Global Early Warning Initiative for the implementation of climate adaptation, Executive action plan 2023–2027*. Geneva: World Meteorological Organization. https://library.wmo.int/viewer/58209/download?file=Executive_Action_Plan_en.pdf

xDEM contributors. (2023). *xDEM*. Zenodo. https://doi.org/10.5281/zenodo.11204531

Xiao, H., Jiang, N., Chen, X., Hao, M., & Zhou, J. (2023). Slope deformation detection using subpixel offset tracking and an unsupervised learning technique based on unmanned aerial vehicle photogrammetry data. *Geological Journal*, *58*(6), 2342–2352. https://doi.org/10.1002/gj.4677

Yang, D., Qiu, H., Quevedo, R. P., Liu, Y., & Glade, T. (2025). Birchgletscher rock-ice avalanche burying the village of Blatten on 28 May 2025, Valais, Switzerland. *Landslides 2025*, 1–9. https://doi.org/10.1007/S10346-025-02656-Y

Zandler, H., Abermann, J., Robson, B. A., Maschler, A., Scheiber, T., Carrivick, J. L., & Yde, J. C. (2025). Deep learning outperforms existing algorithms in glacier surface velocity estimation with high-resolution data – the example of Austerdalsbreen, Norway. *Frontiers in Remote Sensing*, *6*. https://doi.org/10.3389/frsen.2025.1586933

Zhong, Y., Allen, S., Li, D., Corona, C., Zheng, G., Liu, Q., & Stoffel, M. (2025). Unravelling driving conditions of rock and ice avalanches and resulting cascading processes in High Mountain Asia. *Landslides*, *22*(4), 989–1001. https://doi.org/10.1007/s10346-024-02421-7